Designing and Prototyping of PCM based Thermal Energy Storage system.

Muhammad Yousif
muhammad.yousif@tecnico.ulisboa.pt

Instituto Superior Técnico, Universidade de Lisboa, Portugal
October 2019

Keywords: Phase Change Material (PCM), Macro-encapsulations, Temperature-history (T-History), COMSOL Multiphysics, Latent Heat Thermal Energy Storage (LHTES), Submerged spiral type HX.

ABSTRACT – The Phase Changer Materials (PCM) are known to have high heat storage density and low thermal conductivity. In order to validate the use of PCM based Thermal Energy Storage (TES) for district heating purposes, a lab-scale validation site of Latent Heat Thermal Energy Storage (LHTES) is designed and constructed.
The selection of suitable commercially available PCM for the given temperature range is done experimentally using T-history technique. Two types of heat exchangers (HX) are designed; submerged counter flow (consecutive coils are rotated in different orientations) spiral tube HX and diffuser based macro-encapsulated HX. The low thermal conductivity of PCM is overcome by complex mechanical structure of the HX. The selection of macro-encapsulation is done numerically using COMSOL Multiphysics 5.4.
The T-history experiments done in this study show that Crodatherm-60 is the best PCM for the given temperature range (46°C-72°C). Submerged spiral type HX is designed to have counter flow and fins, to improve the heat transfer coefficient. The ellipsoid type encapsulations (HeatStixx) are better than slab type encapsulations (HeatSel), the charging and discharging time of ellipsoid type is almost 60% less than the slab type.
Comparing the two designs, submerged spiral type HX shows almost 58% more storage capacity compared with HeatStixx and 54 % more for HeatSel. But the charging and discharging time of macro-encapsulations is much faster as compared to the spiral design

1. INTRODUCTION

Heating and cooling sector of the European Union makes up more than fifty percent of the total energy demand. Where most of the demand is met by fossil fuels which raise serious environmental concerns and security of supply issues to Europe. By supplying district heating and cooling services, and integrating RES is the only sustainable way, but demand response, the unpredictability of RES and grid balancing are some of the major challenges [1]. Thermal heat storage can increase the efficiency of the overall CHP plants and also provide flexibility in the operation. These storage units store the excess heat when the demand is low and release it when the demand is high, it can charge or discharge depending on the demand profile. The TES system integrated with the CHP enables to provide heat at faster response times and reduces the start/shutdown of the powerplants.
Phase Change Materials (PCM) are used in thermal energy storage units to store low-grade heat (30°C - 250°C). Recently they have gained popularity owing to their environmentally friendly nature, high storage density, availability and their tendency to store heat even at low-temperature differences.
To address this Pump-Heat, a European-Union funded H2020 project was initiated. This project includes two Lab validations one cold and one warm, and one demonstration in IREN, Italy. The lab-scale validation rig is constructed at KTH, Sweden. At first, a suitable PCM is selected after experimental evaluation and then two types of Heat exchanger are designed. A submerged spiral coil HX keeping in mind the design problems encountered in the previous units and a diffuser based filled with commercially available macro-encapsulations. Different types of capsules are simulated and then the best one is selected.

2. LITERATURE REVIEW

2.1. Thermal Energy Storage:

A technology in which energy is stored either by cooling or heating in a storage material and extracted when there is a need for heating and cooling, or energy production is called Thermal Energy Storage (TES). TES can regulate demand profile from short to a long period of time and improve the overall system efficiency. TES is environmentally friendly, less expensive than other storages and has a lot of applications [2]. It is basically divided into two major types; Thermal and Chemical which are further divided into different categories, Figure 1.

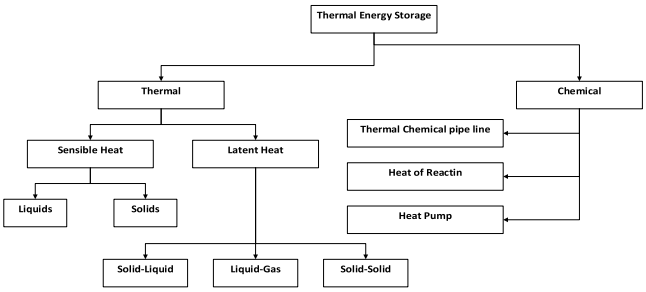

Figure 1: Types of Thermal Energy Storage [2].

2.1.1. Sensible Heat Storage:

Sensible Heat Storage (SHS) is the simplest form of heat storage, in which thermal energy is stored by either decreasing or increasing the temperature. The amount of heat stored depends upon the specific heat capacity of the material and the temperature difference between the source and storage material. Some of the common SHS materials are water, rocks, and sands. With water being the most commonly used and the cheapest option [2].

2.1.2. Latent Heat Storage:

Latent Heat Storage (LHS) is a technology when the heat is being stored during the phase change period. LHS usually has high energy density and can store heat energy for a longer period of time. The amount of heat stored or released depends upon the specific heat capacity and latent heat of fusion [3].

2.2. PCM as a Storage Material:

Recently phase change material has seen a huge amount of potential to be used as heat storage material even for a small temperature difference for a longer period of time [4]. It can store thermal energy for a longer period of time and it is cheaper compared to other similar technologies [2]. However, PCM has some disadvantages such as low thermal conductivity, subcooling and phase separation [5]. There are several types of commercially available PCMs with any given temperature limit, Figure 2 shows the classification of PCMs.

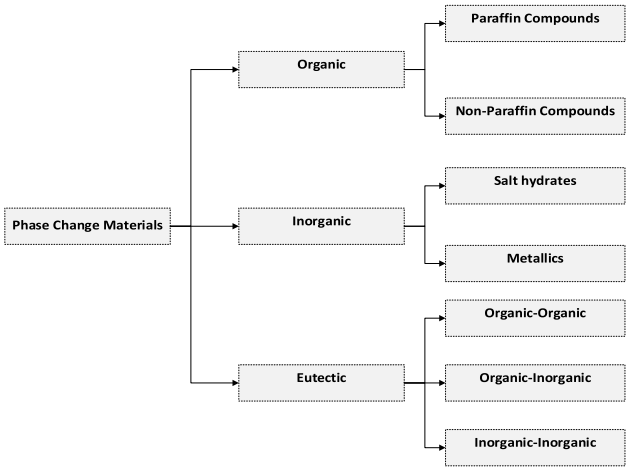

Figure 2: Types of Phase Change Materials [5].

Paraffins and salt hydrates are the most widely used PCMs for LHTES applications. Paraffins proved to be more stable after several thermal cycles compared with salt hydrates. However, they tend to have lower thermal conductivity and enthalpy. On the other hand, Salt hydrates are more prone to corrosion and show sub-cooling during the solidification process [6].

2.3. Types of Heat Exchangers:

In order to integrate PCM as a storage material into the system, a container that will also be used as the heat exchanger is introduced. There is a large variety of heat exchanger containers that can be used for this purpose, but generally, for LHTES submerged HX and diffuser (macro-encapsulation) tanks are preferred depending on the system requirement.

For submerged HXs most commonly heat transfer area and the inlet temperature determines how fast is the charging and discharging process [9], [10]. After experimenting with five different types of HX, the one with the largest heat transfer area has the highest power. But when the comparison is made based on the power per unit area, double pipe with graphite matrix attached to it has the highest value [10]. Some of the recent models are discussed in this chapter.

2.3.1. Spiral Type Heat Exchanger:

A spiral coil heat exchanger was designed and tested in a study [11], the model consisted of eight coils which are counter-flow with any adjacent coils and has four vertical tubes for hot and cold HTF, two at the center and two at the boundary of the tank, as shown in Figure 3. It was encountered in the experimental process that 25 % of PCM was a dead mass, meaning that only the PCM close to the coils is affected by the temperature difference [11].

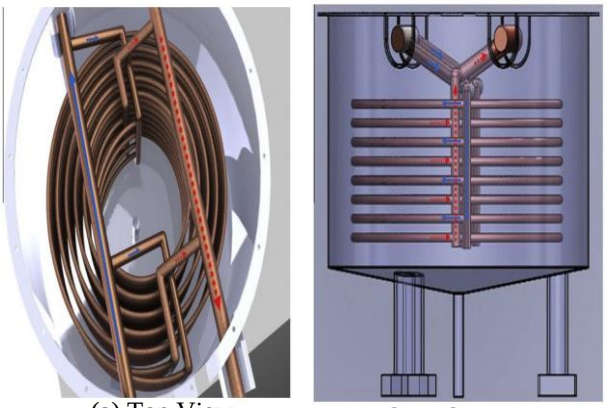

(a) Top View (b) Side View

Figure 3: Spiral Type HX [11].

2.3.2. Straight pipe with spiral fins HX:

Another model of the heat exchanger with straight copper tubes consisting of spiral wire fins was simulated and tested [12], Figure 4. In this study, the HX gives satisfactory results, but the overall heat capacity is decreased owing to the large spiral fin area which reduces the amount of PCM in the HX. Furthermore, it was noticed during the solidification process a layer of solid PCM is attached to the fin area, the thickness of which increases with the solidification process. This layer provides the thermal resistance which will slow down the solidification process. After taking double the time of charging, only 75% of PCM solidifies [12].

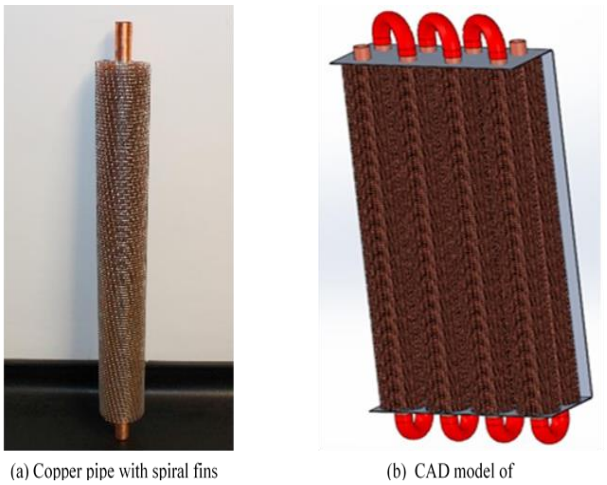

(a) Copper pipe with spiral fins (b) CAD model of

Figure 4: Spiral finned shell and tube HX [12].

2.3.3. U-Tube Shell and Tube Heat Exchanger:

Experimental performance evaluation was performed on vertical U-tube shell and tube heat exchanger [9], in this study horizontal and vertical orientation of the model was tested, as shown in Figure 6. For the charging phase, the horizontal orientation was found to be more effective since it promotes natural convection, while for the discharging it's not that different. It also states that the temperature difference is one of the main driving factors. In the absence of fins, the charging and discharging time will be much higher and PCM in the area close to the boundary of the cylinder will be a dead mass.

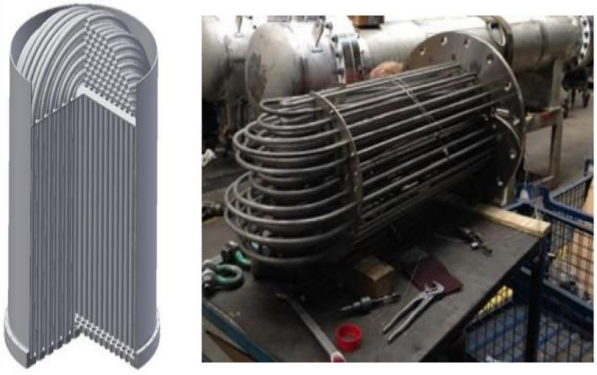

(a) CAD view (b) Real Model

Figure 5: U-Tube shell and tube HX [9].

2.3.4. Macro-Encapsulated Heat Exchanger:

The model of a macro-encapsulated heat exchanger is very simple, capsules (plastic, metal) filled with PCM are added layered into a container having two diffusers, one at the top and one at the bottom. The performance of a macro-encapsulated HX depends on a number of factors; capsule type, shape and size, void fraction, type of PCM, properties of HTF (flow rate, heat transfer coefficient) and tank design [14]. A generic macro-encapsulated tank is shown in Figure 6.

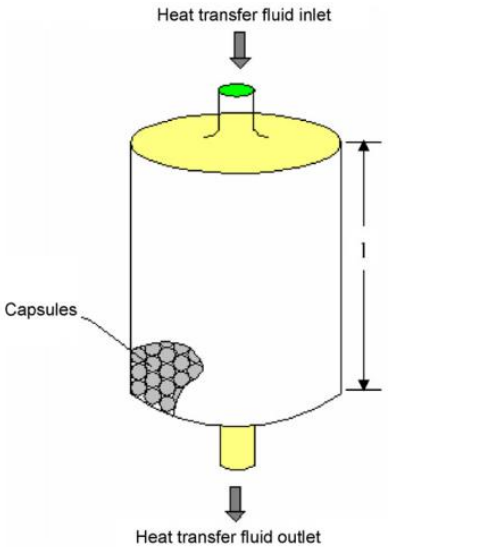

Figure 6: U-Tube shell and tube HX [14] .

2.4. Heat Storage Capacity of PCM storage tank:

The amount of heat stored in a storage tank is a vital parameter when designing an LHTES. The total heat stored is a sum of sensible heat and latent heat. Mostly the heat storage capacity depends upon the mass of PCM and the thermal properties of PCM, such as specific and enthalpy of fusion. The total heat stored in the tank throughout its temperature range is given in the Eq (1), [15].

$$Q = m\,[C_{p,s}(T_m - T_i) + \Delta h_{s-l} + C_{p,l}(T_f - T_m) \quad (1)$$

Where, $C_{p,s}$ and $C_{p,l}$ are the specific heats during their liquid and solid phase, T_i, T_m, and T_f are the initial, melting and final temperatures of a PCM respectively, and Δh_{s-l} is the enthalpy change during the phase change (solid-liquid or Liquid-Solid) or simply called the latent heat of fusion. Mass multiplied by the latent heat of fusion gives the latent heat stored and the rest gives sensible heat stored in the storage tank, [15].

3. METHODOLOGY:

3.1. Storage Material Selection:

Selection of a suitable storage material is one of the most important tasks of this thesis, different types of PCM are evaluated based on different criteria. Some of which are given below [16], [17]:

- High Storage Density
- Good heat conductivity
- Phase Change temperature should be within the operating temperature
- Zero or minimum subcooling

Since this thesis is under the framework of PumpHeat project, the charging temperature of 72°C will be provided by the heating source at IREN [18]. It was noted in the inspection of the heat pump that the heat pump can run at a low evaporator temperature of 46°C. If we take a pinch temperature of 3°C, the operating temperature of TES will be between 49°C and 69°C, as depicted in Figure 7. But to get three times faster discharge rate while operating within these temperature ranges the ideal phase change temperature should at 62.3°C, by using lever rule for the given temperature range. Since the commercially available PCMs do not have a sharp phase change temperature, PCMs having 59±3 °C phase changer temperature will be shortlisted for our application.

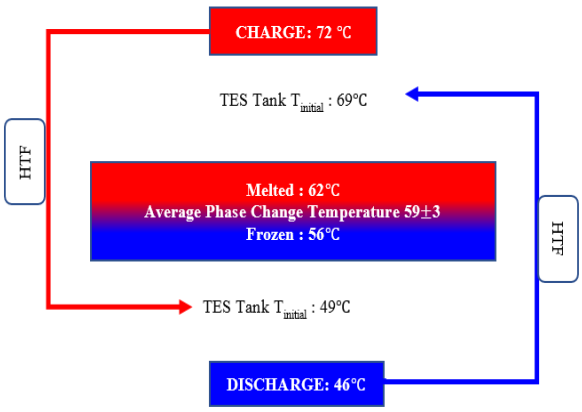

Figure 7: Operating Temperature Range of PUMPHEAT [13].

3.1.1. Shortlisted PCMs:

Keeping in mind the previously described criteria and the

temperature range, five commercially available PCMs were shortlisted. Among them three were organic (Paraffin) and two inorganics (Salt hydrates), RT-60, RT-64HC from Rubitherm; CrodaTherm-60 from CRODA; SU-58 from SunAmp; ATS-58 from Axiotherm. Table 1 shows some of the important characteristics of the shortlisted PCMs, these values were taken from the datasheet provided by the supplier.

Table 1: Shortlisted PCMs

Product Name	Phase Change Temperature (°C)	Heat Storage Capacity (kJ/kg)	Heat Conductivity (W/m. K)
RT-62HC	62 ± 1	230	0.2
RT-64HC	64 ± 2	250	0.2
CrodaTherm-60	60 ± 3	217	0.29
SU-58	58 ± N/A	226	N/A
ATS-58	58 ± 2	240	0.6

3.1.2. Temperature -History Testing:

The properties stated in Table 2 are extracted from the data sheets provided by the suppliers. These thermal properties are very vital for designing the thermal energy storage systems, to have a better idea of available thermal capacity and charging/discharging rates. Most of the values provided by the suppliers are obtained by using traditional evaluation methods such as differential scanning calorimeter (DSC) and differential thermal analysis (DTA). T-history is a recently developed method for evaluating enthalpy and heat capacity which can be used for non-homogeneous samples showing subcooling behavior. Because of this method was used in this study to five shortlisted samples. A short description of this method is given in this study.

3.1.3. Experimental Setup:

The selected PCMs were poured in the Stainless-steel test-tubes after melting them in an electric furnace and then labeled. The reference tube is a solid Stainless-Steel tube with the same dimensions and shape as the test sample was selected. After pouring the materials in the test tube the two thermocouples were placed inside the test tubes and then later insulated using a 19 mm thick High-Temperature Armaflex cover. These insulated tubes were laid down on the test container. This container was then placed in an ACS Hygross 1200 climate chamber, where it was thermally cycled between four heating and cooling cycles respectively between the temperature range of 45°C - 80°C with the ramp of 0.1 K/min, Figure 8. The Schematic of the experimental setup is shown in Figure 9 (a) and the SS tube along with the armaflex insulation is shown in Figure 9 (b) and (c).

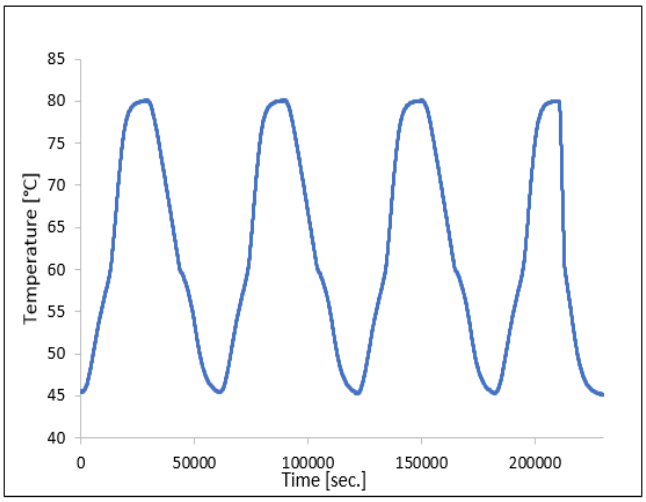

Figure 8: Temperature input to the Climate Chamber

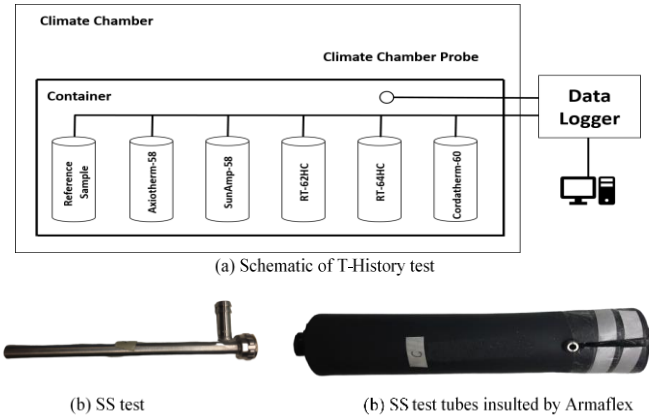

(a) Schematic of T-History test

(b) SS test

(b) SS test tubes insulted by Armaflex

Figure 9: Experimental Setup of T-History

3.2. Heat Storage Tank Design:

Designing a heat storage tank which will also act as a heat exchanger was also an integral part of this study. Given the limitation of the laboratory space few constraints related to the size of the tank were there. Designing and modeling of the tank are done using Solid Edge ST 10, keeping in my all the limitation and requirements, Figure 10. All the measurements are in mm.

This study mostly focuses on the internal part of the tank which will act as a heat exchanging medium. Two different configurations were designed which be placed in the above-mentioned tank: (1) Shell-and-tube spiral type with HTF in the tube and PCM in the shell and (2) Diffuser based with many encapsulations stacked in the tank and water flowing through it.

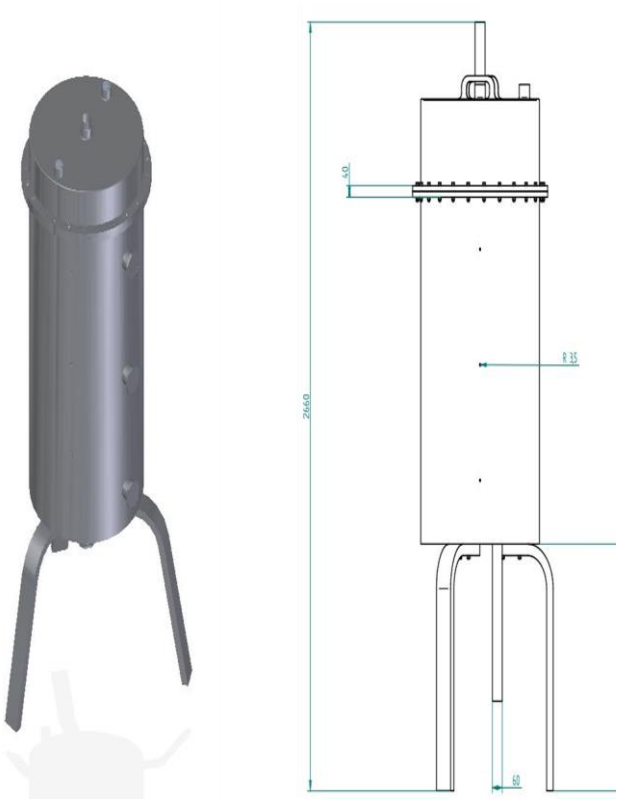

Figure 10: U-Tube shell and tube HX.

3.2.1. Submerged Spiral Type HX Storage:

The first design consisted of two pipes one at the center and the other at the inner periphery of the external tank. The model is oriented vertically, and the spiral copper tubes are placed concentrically to the tank and the center pipe. The HTF will enter from the center pipe and distribute equally among all the spiral tube levels, where after circulating will ultimately exit close to the inner periphery of the outer tank in the side pipe. The number of turns and the pitch between the turns and the different levels correspond to the heat transfer surface and the maximum heat capacity. To keep the balance of heat transfer surface and the heat capacity a pitch of 50 mm was decided for the turns and between the levels.

By putting the pitch of 50 mm between different turns of the coil and the end diameter, an automatic tube having five turns was generated from the Solid Edge. The same procedure was applied to generate different levels of the spiral by inputting the length of the center pipe and the pitch, which resulted in fifteen levels, as illustrated in Figure 11.

But the heat transfer simulations done on the COMSOL for this model which is not part of this study, show that the heat transfer rate was very low. Moreover, since the pitch between the spiral coil was large which resulted in very slow phase change and especially the area close to the center pipe and the boundary of the tank didn't undergo any phase change.

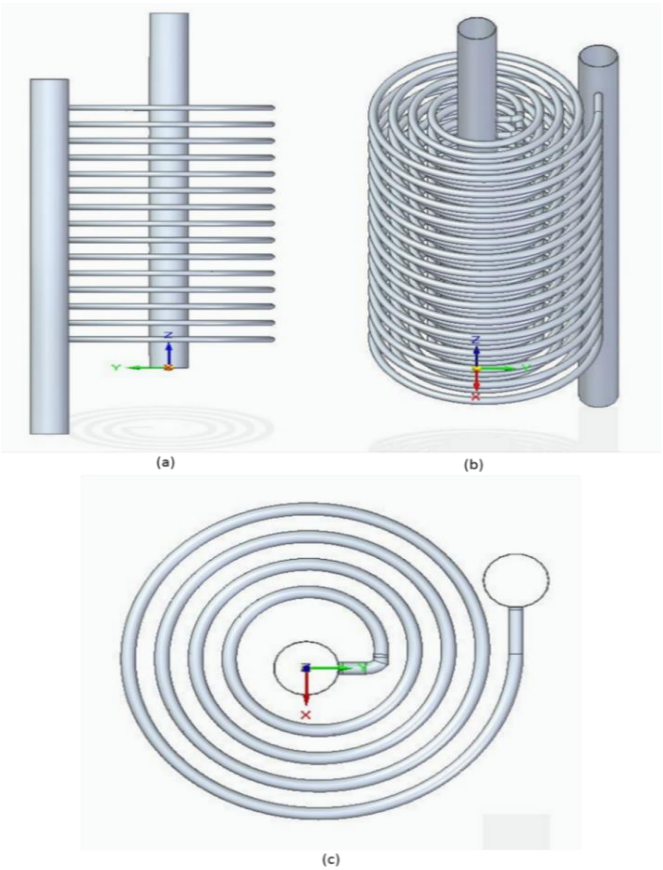

Figure 11: Initial Submerged HX design; (a) Side View, (b) Isometric view and (c) Top view

3.2.1.1. Final Design:

After looking at the constraints and talking with the suppliers, changing the orientation of the inner structure and decreasing the pitch between the turns to 40 mm and among different levels to 35 mm is the easiest and the most efficient way. The main idea behind this new design was to utilize all the space within the tank effectively and to have a counter-flow which will increase the heat transfer area. Now there were three pipes instead of two, one at the center and another two at the opposite sides of the inner periphery of the tank. And the coils were not anti-clockwise in direction anymore, in fact, it was a mixture of clockwise and anti-clockwise.

The same procedure was applied to get the number of turns and the number of spiral levels, which resulted in eight turns and thirty-six levels, Figure 12. Holes were generated on either side of the center pipe with the first hole on the left side and the second one on the right side which are 35 mm apart vertically. The first row starts from the left side of the center pipe and rotates in an anti-clockwise direction Figure 12(a), while the second row starts from the right side and rotates in a clockwise direction. In the third and fourth row, the pattern is reversed, with third-row starting from the left side and rotating in a clockwise direction and the fourth row starting from the right side rotating in an anti-clockwise direction. After this the pattern of four levels is repeated for nine times making thirty-six levels, as visible in Figure 12 where the side view of the final structure is presented.

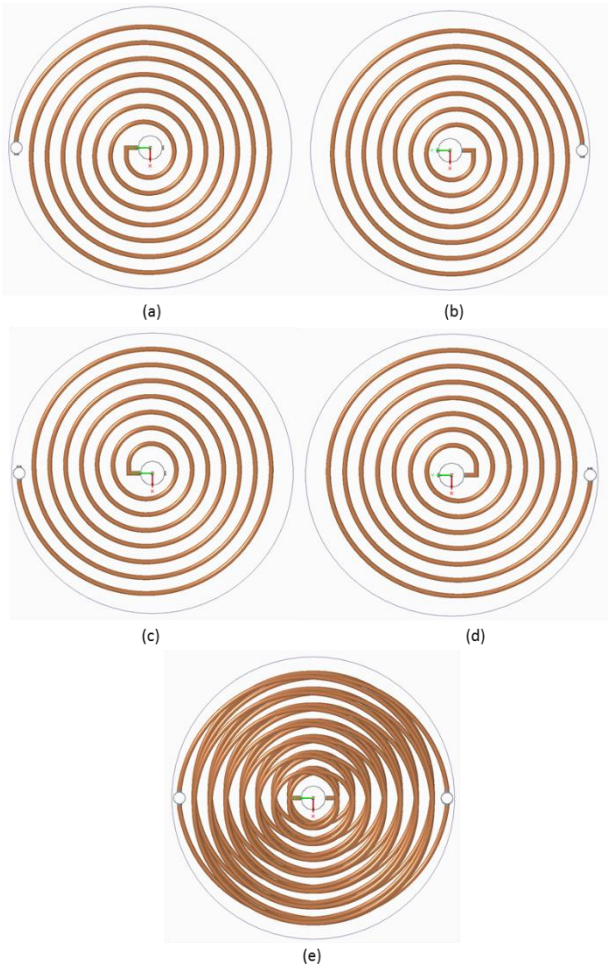

Figure 12: Top view of final inner version; (a) First row, (b) Second row, (c) Third row, (d) Fourth row and (e) Top view

3.2.2. Encapsulated Tank Design:

The designing and modeling of macro-encapsulated PCM storage tank was also part of this study in which various marco-encapsulation options were analyzed and simulated. The size and shape of the encapsulation play a vital role in the performance of LHTES. Larger encapsulations will have higher thermal energy storage capacity but the charging and discharging rate will be much slower, while in smaller encapsulations the rate of charging and discharging faster but they have much lower thermal energy storage capacity [22]. According to the study done previously on this project, it was suggested that capsules of 60 mm height and 30 mm diameter will be suitable for the given working temperature range [18]. To find a suitable supplier who could provide these custom-made capsules was an impossible task, the only option was to manufacture them in the lab using 3-D printers. One 3-D printer was also bought for this purpose, but then after doing some estimations, it was clear that 3-D printer will take approximately five to six months to produce the required number of capsules if run continuously without any interruption. Moreover, Polylactic Acid (PLA) which the printing material has a melting temperature between 150 to 160 °C, but there may be deflection in the shape due to heat at a much lower temperature of around 60°C [23].

Now the only option left was to have something which was commercially available in the market. Two types of commercially available marco-encapsulation provided by Axiotherm GmbH were analyzed using COMSOL Multiphysics 5.4 to check their performance under the given conditions because there is no performance evaluation data available.

3.2.2.1. Simulation Model Setup:

This section will explain how the encapsulations are modeled and the procedure through which different material properties were set up in the simulation. SpaceClaim Direct Modeler (SCDM 2019) is used to model the encapsulations and COMSOL Multiphysics 5.4 is used to study the heat transfer inside these encapsulations. Some groves and cuts were ignored during the modeling for the sake of simplicity.

Two-dimensional study of these encapsulations is not enough, to fully study the behavior of these encapsulations a three-dimensional study is performed using heat transfer physics in a time-dependent study. Heat transfer study in COMSOL is not based on enthalpy rather it is based on heat transfer coefficient, specific heat capacity, thermal conductivity and density of the material. The physical properties of both the cover and PCM are temperature dependent. The physical properties of the cover which is poly-propylene can be obtained from the built-in material library in the COMSOL. Initially both the cover and PCM are kept at 49°C (322 K) and a heat flux having heat transfer co-efficient of 123 $W/m^2.K$ at 72°C (345 K) is applied at the boundary of the capsule to check the performance, Equation, which is then run for a period of two hours with physically controlled time interval. The values for the PCM were added manually using the data sheets and the T-history measurements.

3.2.2.2. HeatStixx (Ellipsoidal Shaped):

First encapsulation was shaped like an ellipsoid with several groves engraved in the model known as HeatStixx. The capsule has a diameter of 0.04 m and a length of 0.3 m, whereas the volume of 245 mL was measured manually at the lab. The model is basically a simplified version of the capsule, where the small cuts and groves are neglected for the sake simplicity except the two deeper ones on either side. The model used for computation and the meshing is shown in Figure 13.

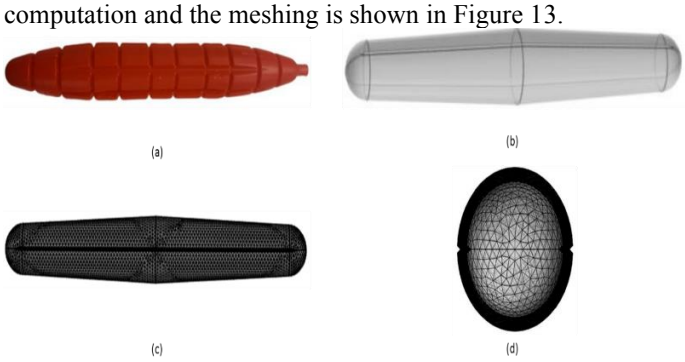

Figure 13: Illustration of HeatStixx; (a) HeatStixx capsule, (b) Approximated CAD model, (c) Side view in computational model, and (d) Top view in computational model

3.2.2.3. HeatSel (Slap with curved edges):

The second encapsulation is somewhat similar to a slab with curved edges having several cuts diagonally and bisectionally, known as HeatSel. It has a height and length of almost 0.2 m and an internal volume of 350 mL. The thickness of this slap is different along the length which can be seen from cross-sectional view in Figure 14 (d). An approximated 3-D model and the meshing of a cross-section is shown in Figure 14.

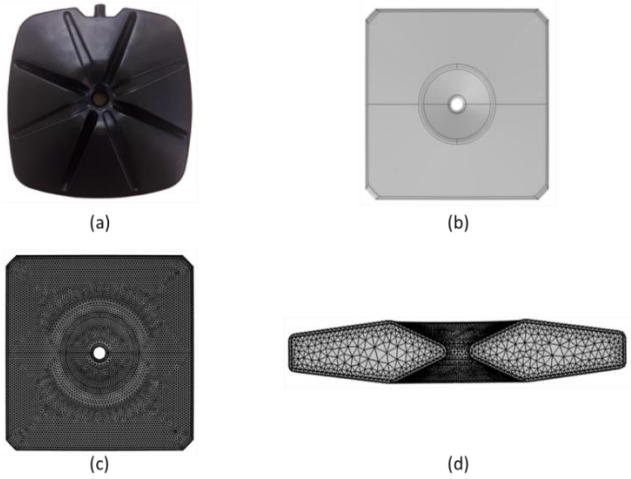

Figure 14: Illustration of HeatSel; (a) HeatSel capsule, (b) Approximated CAD model, (c) Top view in computational model, and (d) Cross-sectioned view in computational model

3.3. Lab Rig Setup:

A lab-scale PumpHeat validation site is constructed at KTH, Sweden for testing LHTES performance. The existing auxiliary setup consists of heating devices (Heat Pump, Electric Heater), tanks (thermal storage tank, Hot and Cold inertia tanks), directional valves and measurement devices (T-Type thermocouples, Resistance Temperature Detectors, flowmeters, and differential pressure transmitter).

During the charging phase, an electric heater (labeled as H in Fig.15) which is controlled by PID supplies the exact amount of heat needed to water (which acts as an HTF), to reach a user-defined temperature point. And the centrifugal pump (P-1) adjusts the speed to deliver water at the required flowrate. While during the discharging phase the heat from the heat storage tank is released in the atmosphere by using a fin-and-coil heat exchanger (labeled as Q, Fig.15). To avoid temperature fluctuations in the HTF, both hot and cold inertia tanks are filled with water at a set temperature. Currently, the heat pump is not in use since the temperature requirement is completed through an electric heater.

Most of the auxiliary system remains the same as used previously for testing Macro-Encapsulations in [24]. Only two changes are made; first, the new storage units are installed and second, an additional hydraulic loop is added to accommodate the new storage unit through a three-way directional valve without disturbing that the existing configuration is not disturbed.

To control the proportion of water inlet and outlet to the tank, a three-way valve integrated with a temperature-regulating module is installed. Two inlet pipes are also added to accommodate the new submerged heat exchanger design as discussed in section 3.2.1 of this study. A temperature sensor (TC10/TC11) and a pressure-drop regulating valve (B1/B2) is placed on each inlet pipe [25]. To measure the temperate throughout the storage tank, eleven T-type thermocouples and nine resistance temperature detectors (PT-100) are installed.

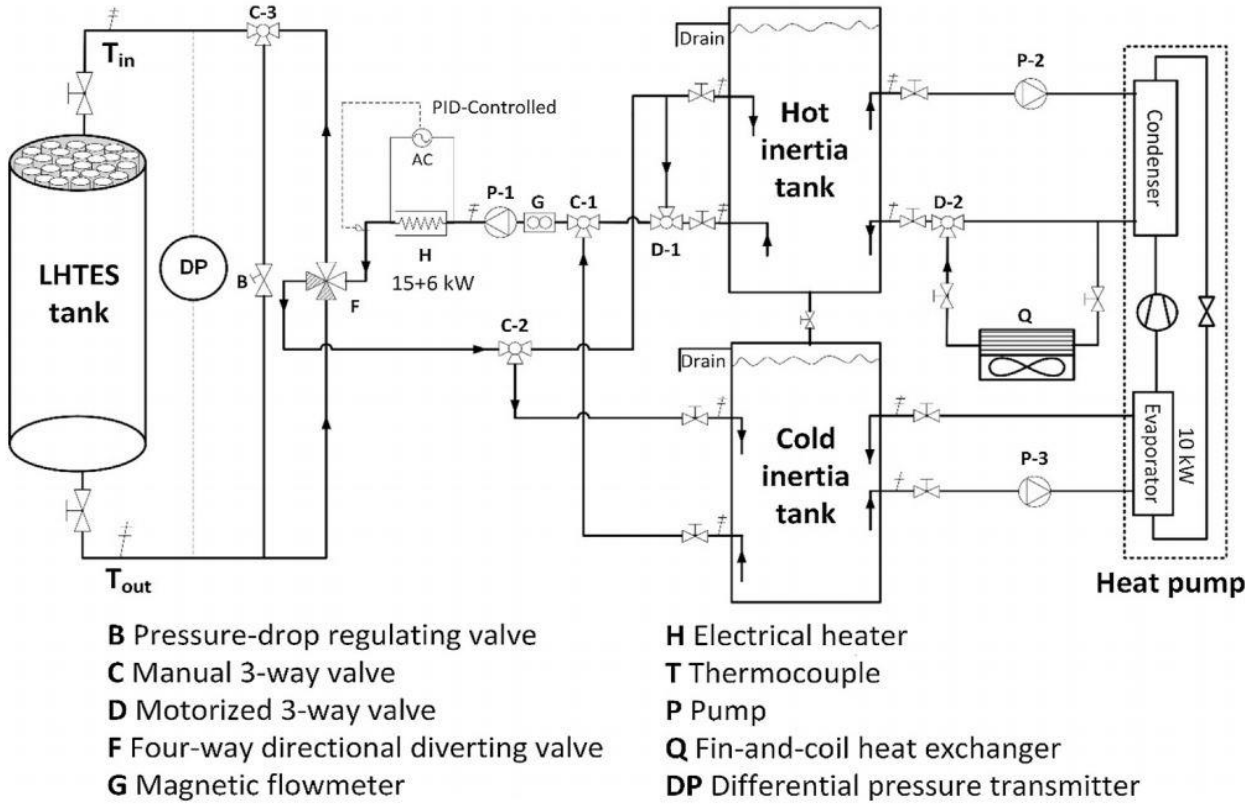

Figure 15: Schematic of Lab Validation site [24]

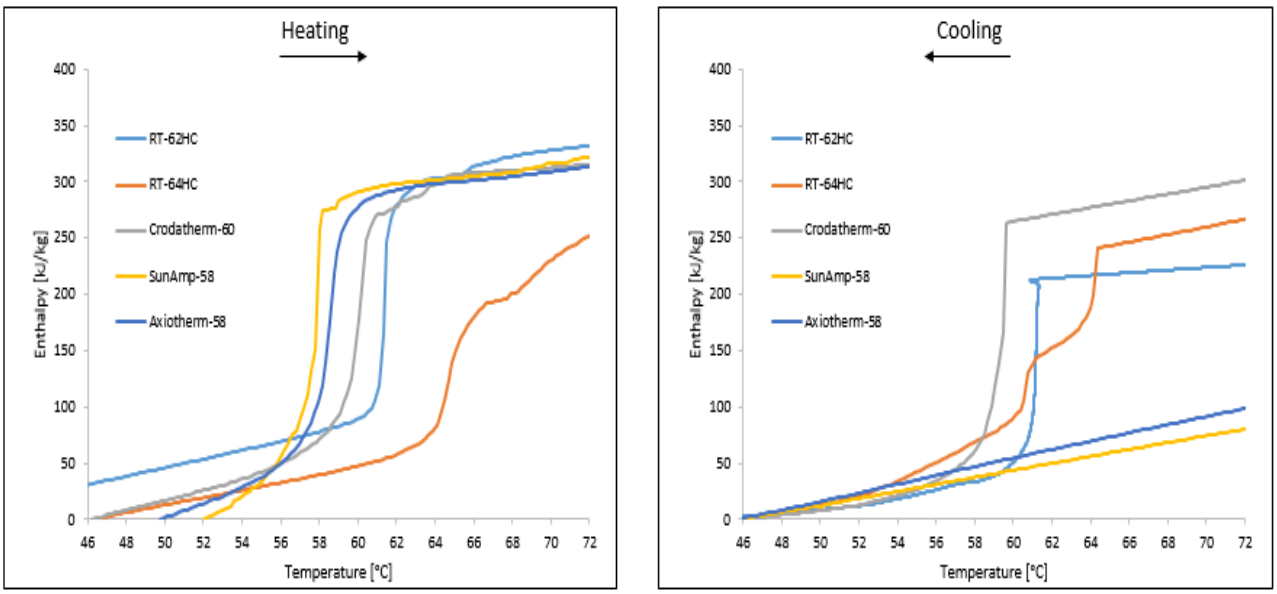

Figure 16: T-History results of Selected PCMs

4. Results and Discussion:

4.1. Results of Material Selection:

The data obtained from the Climate chamber was then filtered and analyzed using VBA (Visual Basic in Applications) in excel sheets. The data was divided into five different heating and cooling cycles. The enthalpy of each test sample is plotted against temperature, Figure 16, for heat and cooling of the second cycle respectively.

Instability and uncertainty are seen among the two salt-hydrate PCMs, namely Axiotherm-58 and SunAmp-58. During the second melting cycle, they easily liquify as seen from the enthalpy Figure 16, but during the solidification, both of them don't solidify and the latent enthalpy is also absent Figure 16. This later continues to further cycles where these two samples do not even liquify completely. Furthermore, salt hydrates are also degraded with the passage of time due to phase separation. To avoid this problem these two are discarded. Among the three paraffin samples RT-64HC exhibit two-phase change stages in both heating and cooling cycles as seen in the graph, Figures [16], one at 64°C and another close to 70°C for heating cycle and for cooling cycle at 60 °C and 64°C, indicating that the material is not pure and is non-homogenous. This will increase the charging/discharging temperature range which is less desirable for LHTES systems. Moreover, 64°C is very high for district water heating applications because it may lead to partial charging and discharging when used in an LHTES. Crodatherm-60 and RT-62HC were the best candidates, Crodatherm-60 had the higher enthalpy change (316 kJ/kg) for a given the temperature range and the heat capacity was noticed to be the highest among the test samples.

4.2. Result of COMSOL simulations:

The objective of performing the simulation is to check whether the complete PCM inside these encapsulations have a phase change. Moreover, identifying the areas inside the encapsulations where the melting and freezing is difficult to achieve is also part of this study. There are two major criteria is selecting a suitable encapsulation. One is to have a fast charging and discharging process, and the second is to have a complete phase change throughout the PCM volume inside the capsule. For this purpose, the average PCM temperature and the encapsulation are potted against the time, and the cross-sectional view showing the temperature profile is presented in this study.

4.2.1. HeatStixx Result:

According to the results obtained from COMSOL, the average PCM temperature reaches the phase change temperature after almost 1000 seconds (16 minutes), hence starting the phase change process, Figure 17. But it is evident from the cross-sectional temperature profile of the model that the temperature is quite low around the axis and the center of the geometry. This area can be seen in Figure 18 (b). Regardless after 7200 seconds (2 hours) the average PCM temperature reaches the final temperature. Moreover, the cross-sectional temperature profile also shows that the temperature even in the hardest areas to melt/freeze region almost reaches 344 K (71°C). It is very safe to say that the phase change takes place throughout the volume of the capsule.

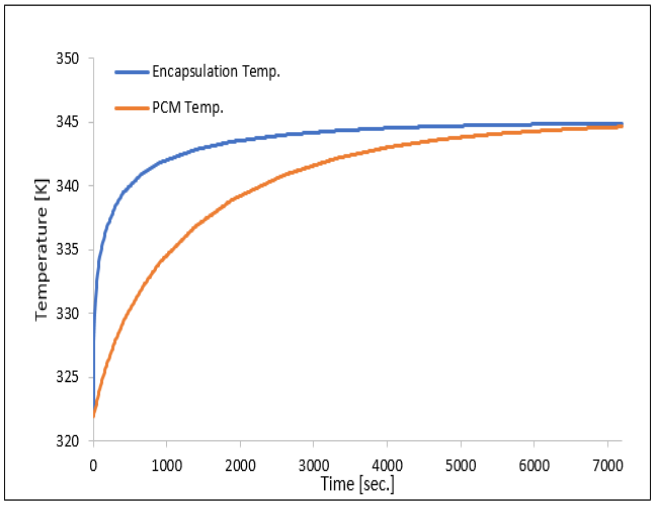

Figure 17: Temperature vs. Time for HeatStixx

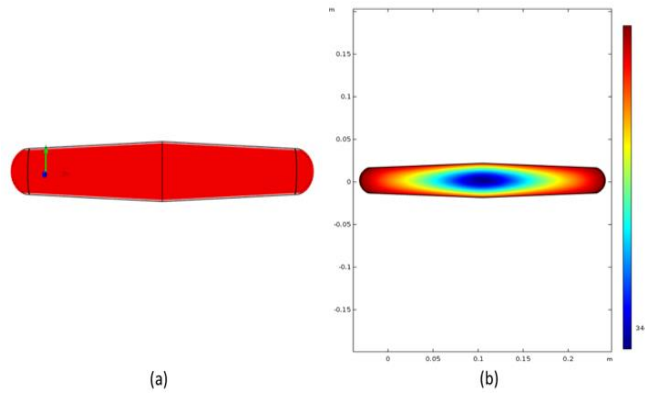

Figure 18: Results from COMSOL; (a) Cut view of the capsule, (b) Cross-sectional temperature profile

4.2.2. HeatSel Result:

The graph presented in Fig.19 shows that the average PCM temperature in the capsule reaches the phase change temperature around 2700 seconds (45 minutes). However, the cross-sectional temperature profile clearly indicates the areas where the temperature difference is much lower, Figure 20 (b). This area is close to the center of the geometry where the thickness of the capsule is also greater. The average PCM temperature reaches 342 K (69°C) after 7200 seconds (2 hours), but the cross-sectional temperature profile indicates some regions where the phase change process just begins at the end of the two hours. The temperature in some regions is as low as 334 K (61°C) because of the capsule thickness in that part, which is highly undesirable. Figure 20 (b) shows the slice in the geometry and the regions which are difficult to melt and solidify during the charging and discharging phase respectively.

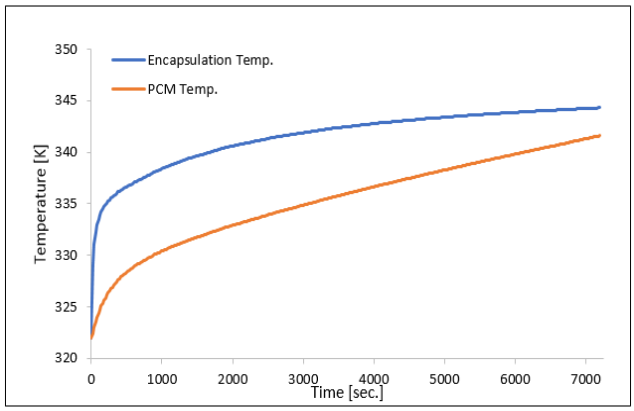

Figure 19: Temperature vs. Time for HeatSel

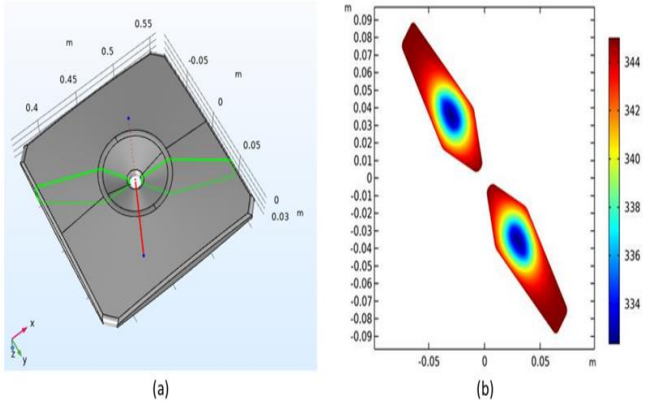

Figure 20: Results from COMSOL; (a) Cut view of the capsule, (b) Cross-sectional temperature profile

4.3. Total Heat Stored in the Storage Tank:

The total amount of heat stored (Latent and Sensible) in the heat exchange can be calculated using the Eq. (1). The mass of the PCM is calculated by subtracting the volume of the inner structure (Spiral tubes and pipes) with the total volume of the tank for the Submerged Spiral type HX, which is then multiplied by the density of the PCM to get the exact mass. For the macro-encapsulation ones, the packing factor provided by the supplier is used to calculate the mass of PCM. The total heat stored, and its classification is shown in Table 2.

Table 2: Total Heat Stored

Parameter	Type of Heat Exchanger		
	Submerged Spiral type HX	HeatStixx	HeatSel
Sensible Heat stored (kJ)	12025.69	4931.85	5240.51
Latent Heat stored (kJ)	124594.00	51097.20	54295.10
Total Heat stored (kJ)	136619.70	56029.05	59535.60

5. Conclusions:

After analyzing the results in section 4.2. of this study, it is decided that Crodatherm-60 is the best candidate for this LHTES unit at the given temperature conditions. Crodatherm-60 is thermally very stable and the enthalpy change is also the highest. Furthermore, it is cheaper, non-toxic and non-corrosive nature makes it a perfect candidate for submerged HX.

The spiral submerged HX configuration designed in this study addresses the dead mass PCM problem which was encountered in the previous designs. Moreover, counterflow among different levels and the addition of fins greatly affects the thermal conductivity of the over the system.

Results of the first-ever simulations done on Axiotherm macro-encapsulations in section 4.2., prove that the heatstixx is far better than the HeatSel encapsulations based on the criteria defined earlier. Heatstixx reaches the phase change temperature almost after 16 minutes whereas HeatSel takes almost 45 minutes to reach the same temperature. Furthermore, after the two-hour period, HeatSel will still have PCM which has not undergone a phase change, whilst in HeatStixx the whole volume of PCM undergoes phase change. Even though price was not the criteria for the selection, it must be noted that HeatStixx is half the price of the HeatSel, and it is also much easier to stack the rods like HeatStixx in the storage tank rather than the slab-like HeatSel.

The submerged spiral type HX can store almost 57 % more heat compared to the HeatStixx and 52 % more compared to the HeatSel. But the spiral HX is known to have a very high charging time whereas, the HeatStixx charge fully charges in almost an hour and HeatSel takes slightly more than two hours. The discharging of all these HXs is much faster. Furthermore, almost 90 % of the total heat stored is Latent heat in all three cases.

6. Future Works:

The Lab Validation rig is almost ready for preliminary

testing, due to time constraints it is not included in this study. Detailed testing of the LHTES system will be done during the next six months. The detailed simulation of spiral type HX can be done to check the effects of decreasing the pitch and counter flow assembly. Moreover, the experimental data received from the experiments can be compared with the simulations to have a better understanding of the approximations which can be taken during the construction of the next LHTES.

7. References:

[1] N. ITKONEN, Anna-Kaisa BOCKSTALLER, "Towards a smart, efficient and sustainable heating and cooling sector," *Towards Energy Union: the Commission presents sustainable energy security package*, 2016. [Online]. Available: https://europa.eu/rapid/press-release_MEMO-16-311_it.htm. [Accessed: 21-Aug-2019].

[2] I. Sarbu and C. Sebarchievici, "Thermal Energy Storage," in *Solar Heating and Cooling Systems*, Elsevier, 2017, pp. 99–138.

[3] L. F. Mehling, Harald Cabeza, *Heat and cold storage with PCM - An up to date introduction into basics and applications*, First. Berlin: Springer-Verlag Berlin Heidelberg, 2008.

[4] J. Pereira da Cunha and P. Eames, "Thermal energy storage for low and medium temperature applications using phase change materials - A review," *Appl. Energy*, vol. 177, pp. 227–238, 2016.

[5] A. Sharma, V. V. Tyagi, C. R. Chen, and D. Buddhi, "Review on thermal energy storage with phase change materials and applications," *Renew. Sustain. Energy Rev.*, vol. 13, no. 2, pp. 318–345, 2009.

[6] W. S. Andreas Heinz, "Application of Phase Change Materials and PCM slurries for thermal energy storage," in *Ecostock Conference 2006 - Proceeding*, 2006.

[7] L. F. Zalba, B, Marin J, Cabeza and H. Mehling, *Review on Phase changing materials to store energy*, vol. 23. 2003.

[8] R. Pilar, L. Svoboda, P. Honcova, and L. Oravova, "Study of magnesium chloride hexahydrate as heat storage material," *Thermochim. Acta*, vol. 546, pp. 81–86, 2012.

[9] H. A. Zondag, R. de Boer, S. F. Smeding, and J. van der Kamp, "Performance analysis of industrial PCM heat storage lab prototype," *J. Energy Storage*, vol. 18, no. October 2017, pp. 402–413, 2018.

[10] M. Medrano, M. O. Yilmaz, M. Nogués, I. Martorell, J. Roca, and L. F. Cabeza, "Experimental evaluation of commercial heat exchangers for use as PCM thermal storage systems," *Appl. Energy*, vol. 86, no. 10, pp. 2047–2055, 2009.

[11] A. López-Navarro *et al.*, "Performance characterization of a PCM storage tank," *Appl. Energy*, vol. 119, pp. 151–162, 2014.

[12] W. Youssef, Y. T. Ge, and S. A. Tassou, "CFD modelling development and experimental validation of a phase change material (PCM) heat exchanger with spiral-wired tubes," *Energy Convers. Manag.*, vol. 157, no. October 2017, pp. 498–510, 2018.

[13] Justin NW Chiu, "D3.4 – 'Design and Specifications of Warm Temperature Thermal Storage,'" Stockholm, 2019.

[14] A. F. Regin, S. C. Solanki, and J. S. Saini, "Heat transfer characteristics of thermal energy storage system using PCM capsules: A review," *Renew. Sustain. Energy Rev.*, vol. 12, no. 9, pp. 2438–2458, 2008.

[15] K. Nithyanandam, J. Stekli, and R. Pitchumani, "High-temperature latent heat storage for concentrating solar thermal (CST) systems," in *Advances in Concentrating Solar Thermal Research and Technology*, Elsevier, 2017, pp. 213–246.

[16] N. Vitorino, J. C. C. Abrantes, and J. R. Frade, "Quality criteria for phase change materials selection," *Energy Convers. Manag.*, vol. 124, pp. 598–606, 2016.

[17] A. Shukla, K. Kant, and A. Sharma, "Solar still with latent heat energy storage: A review," *Innov. Food Sci. Emerg. Technol.*, vol. 41, pp. 34–46, 2017.

[18] CLAUGER, "D3.2 – 'Assessment of Different Options for Thermal Storage in PHCCs,'" 2018.

[19] J. N. W. Chiu and V. Martin, "Submerged finned heat exchanger latent heat storage design and its experimental verification," *Appl. Energy*, vol. 93, pp. 507–516, 2012.

[20] S. N. Gunasekara, R. Pan, J. N. Chiu, and V. Martin, "Polyols as phase change materials for surplus thermal energy storage," *Appl. Energy*, vol. 162, pp. 1439–1452, 2016.

[21] B. Sandnes and J. Rekstad, "Supercooling salt hydrates: Stored enthalpy as a function of temperature," *Sol. Energy*, vol. 80, no. 5, pp. 616–625, 2006.

[22] T. E. Alam, J. S. Dhau, D. Y. Goswami, and E. Stefanakos, "Macroencapsulation and characterization of phase change materials for latent heat thermal energy storage systems," *Appl. Energy*, vol. 154, pp. 92–101, 2015.

[23] J. T. Wertz, T. C. Mauldin, and D. J. Boday, "Polylactic acid with improved heat deflection temperatures and self-healing properties for durable goods applications," *ACS Appl. Mater. Interfaces*, vol. 6, no. 21, pp. 18511–18516, 2014.

[24] T. Xu, J. N. Chiu, B. Palm, and S. Sawalha, "Experimental investigation on cylindrically macro-encapsulated latent heat storage for space heating applications," *Energy Convers. Manag.*, vol. 182, no. December 2018, pp. 166–177, 2019.

[25] J. N. Xu, Tianhao Chiu, "D3.5 – 'Thermal Storage Prototypes to Demo site and to Validation Sites,'" Stockholm, 2019.